doi:10.1016/j.jmb.2007.03.078 J. Mol. Biol. (2007) 369, 1041–1051

JMB

Available online at www.sciencedirect.com

ScienceDirect

ELSEVIER

The Mechanism of Inhibition of Antibody-based Inhibitors of Membrane-type Serine Protease 1 (MT-SP1)

Christopher J. Farady[1], Jeonghoon Sun[2], Molly R. Darragh[1] Susan M. Miller[1] and Charles S. Craik[1,2]*

[1]*Graduate Group in Biophysics University of California San Francisco, 600 16th St. Genentech Hall, San Francisco CA 94143, USA*

[2]*Department of Pharmaceutical Chemistry, University of California, San Francisco 600 16th St. Genentech Hall San Francisco, CA 94143, USA*

**Corresponding author*

The mechanisms of inhibition of two novel scFv antibody inhibitors of the serine protease MT-SP1/matriptase reveal the basis of their potency and specificity. Kinetic experiments characterize the inhibitors as extremely potent inhibitors with K_I values in the low picomolar range that compete with substrate binding in the S1 site. Alanine scanning of the loops surrounding the protease active site provides a rationale for inhibitor specificity. Each antibody binds to a number of residues flanking the active site, forming a unique three-dimensional binding epitope. Interestingly, one inhibitor binds in the active site cleft in a substrate-like manner, can be processed by MT-SP1 at low pH, and is a standard mechanism inhibitor of the protease. The mechanisms of inhibition provide a rationale for the effectiveness of these inhibitors, and suggest that the development of specific antibody-based inhibitors against individual members of closely related enzyme families is feasible, and an effective way to develop tools to tease apart complex biological processes.

Keywords: antibody; standard mechanism protease inhibitor; specificity; serine protease; HuCAL

Introduction

Of the 22 families of naturally occurring, protein-based protease inhibitors known to inhibit the S1 clan of serine proteases, 18 use an identical mechanism of inhibition.[1] Standard mechanism (also known as canonical, or Laskowski mechanism) inhibitors all insert a reactive loop into the active site of the protease, which binds in an extended β-sheet in a substrate-like manner.[2] While some of these inhibitors have developed secondary mechanisms,[3] the primary mechanism of inhibition is extremely well conserved; so much so that crystal structures of unrelated inhibitors overlay perfectly in the protease active site.[4] As evidenced by this remarkable example of convergent evolution, the standard mechanism is an efficient, robust way to inhibit serine proteases. However, this robustness often comes at the expense of specificity. With the exception of a small number of parasitic anti-thrombin inhibitors that also bind to protease exosites,[5] the majority of standard mechanism protease inhibitors have a relatively broad specificity. For example, bovine pancreatic trypsin inhibitor (BPTI) inhibits efficiently almost all trypsin-fold serine proteases with P1-Arg specificity, but can inhibit chymotrypsin (P1-Phe specificity) with a K_I of 10 nM.[6]

Much effort has been expended on the development of specific protease inhibitors for use both as biological tools and as potential therapeutic agents. As attempts to make specific small molecules have beset by difficulties,[7] researchers have often attempted to gain specificity using peptide or protein-based scaffolds. Constrained peptide phage display libraries have yielded extremely potent exosite inhibitors of factor VIIa,[8,9] and standard mechanism inhibitors of chymotrypsin,[10] and urokinase-type plasminogen activator (uPA),[11] with moderate potency and specificity. An alternate approach has

Present address: J. Sun, Amgen Inc., Thousand Oaks, CA 91320, USA.

Abbreviations used: BPTI, bovine pancreatic trypsin inhibitor; uPA, urokinase-type plasminogen activator; scFv, single-chain variable fragment; MT-SP1, membrane-type serine protease 1; HuCAL, human combinatorial antibody library; pNA, *para*-nitroanilide; pAB, *p*-aminobenzamidine; ESI, electron spray ionization.

E-mail address of the corresponding author: craik@cgl.ucsf.edu

been to improve the specificity of naturally occurring protease inhibitors.[12–14] For example, maturation of Alzheimer's amyloid β-protein precursor inhibitor Kunitz domain, a canonical serine protease inhibitor, *via* competitive phage display improved its specificity for factor VIIa by increasing its K_I against a panel of some related serine proteases by two to five orders of magnitude.[13] A third approach has been to mature specific protease inhibitors on other natural protein scaffolds, such as ankyrin repeats or antibodies.[15] Until now, the characterized protease antibody inhibitors have been monoclonal antibodies raised from hybridomas, and have tended towards two types of inhibitors; those that interfere with multimerization (and thus activation) of the protease,[16–18] and those that bind to loops and protein–protein interaction sites[19–22] and occlude substrate binding, instead of interfering with the catalytic machinery of the enzyme, and ensuring complete inhibition.[23]

Earlier, we reported the development of single-chain variable fragment (scFv) antibody inhibitors of the serine protease membrane-type serine protease 1 (MT-SP1).[24] MT-SP1 (also called matriptase) was discovered and cloned in a search for serine proteases expressed in the PC-3 prostate cancer cell line,[25] and was determined independently to be a highly expressed protease in breast cancer tissue.[26] Work by a number of groups has since shown that MT-SP1 may be a key upstream factor involved in the ECM remodeling, and in signal transduction cascades involved in cell transformation.[27] Ablation of MT-SP1 activity has been shown to decrease the invasiveness of both ovarian and prostate tumor cells, and modest orthotopic over-expression of MT-SP1 in mouse epidermal tissue led to spontaneous squamous cell carcinomas,[28] further cementing the role of MT-SP1s in cancer, and suggesting the enzyme is causally involved in malignant transformation.

Here, we have characterized the mechanism of inhibition of the two most potent scFv inhibitors of MT-SP1, E2 and S4. The inhibitors were selected from a fully synthetic human combinatorial antibody library in the scFv format (HuCAL, MorphoSys AG). HuCAL-scFv contains consensus frameworks with diversified light and heavy chain CDR3 regions reflecting the natural human amino acid composition.[29] A combination of mutagenesis experiments, steady-state kinetics, and stopped-flow kinetics reveal that, while the inhibitors gain specificity by making a number of critical interactions with surface loops on the protease, they can be standard mechanism inhibitors, which insert a reactive loop in a substrate like manner into the active site of the protease. This work suggests that an antibody scaffold can be used to create extremely specific standard mechanism protease inhibitors. Furthermore, the design of inhibitors that utilize macromolecular recognition factors (variable loops, protein–protein interaction sites) can help to differentiate highly homologous proteases, and can thus impart specificity upon the inhibitors.

Results

Earlier, we described the maturation and initial characterization of a number of scFv inhibitors of MT-SP1.[24] The scFvs bound tightly to the catalytic domain of MT-SP1, and showed a high degree of specificity, as they showed no appreciable inhibition of a panel of closely related serine proteases, including factor Xa, thrombin, kallikrein, tissue plasminogen activator (tPA), and uPA at inhibitor concentrations of 1 μM. Here, we characterize the mechanism of inhibition of E2 and S4, the two most potent members of this novel class of serine protease inhibitors.

Steady-state kinetics

Previous experiments showed that E2 and S4 had K_D values of 160 pM and 500 pM (as determined by surface plasmon resonance), and were potent inhibitors of MT-SP1. In the current study, a number of steady-state kinetic experiments were performed in an attempt to understand the mechanism of inhibition of these inhibitors. The results of these experiments are summarized in Table 1. Double reciprocal plots revealed that both E2 and S4 are competitive inhibitors of MT-SP1 with respect to Spectrazyme-tPA, a small molecule *para*-nitroanilide (pNA) substrate of P1 arginine serine proteases. To further characterize the tight-binding nature of these inhibitors, accurate K_I values were determined; E2 and S4 are extremely tight-binding competitive inhibitors of MT-SP1, with K_I values of 8.0(±1.3) pM and 140(±6.0) pM, respectively.

To verify that the mode of inhibition is similar in the context of a macromolecular substrate, a discontinuous assay was developed to measure the activation of uPA. The K_M of uPA as a substrate for MT-SP1 was determined to be 1.7(±0.2) μM, and the k_{cat} of MT-SP1 activation of sc-uPA was 0.89(±0.09) s^{-1}. Double reciprocal plots showed that the inhibitors were indeed competitive with respect to macromo-

Table 1. Kinetic parameters of scFv inhibitors

	k_{on}[a] ($10^6 M^{-1}s^{-1}$)	k_{off}[a] ($10^{-3}s^{-1}$)	K_d[a] (nM)	Mode of inhibition	K_I (pM)	Macromolecular MOI	Macromolecular K_I (pM)
E2	2.1	0.38	0.16	Competitive	8.0±1.3	Competitive	12
S4	11.5	5.8	0.51	Competitive	140±6	Competitive	160

MOI, mode of inhibition.
[a] Values determined by SPR.[24]

lecular substrates. From these data, approximate K_I values of 12 pM for E2 and 160 pM for S4 could be extrapolated (Table 1). Since the substrate (uPA) concentration could not be increased above K_M, the errors associated with K_I values are large; nonetheless, they confirm that the inhibitors inhibit MT-SP1 equally well, regardless of the size of the protease substrate.

Pre-steady-state kinetics

A closer examination of the progress curves of the steady-state reactions when enzyme was added to a mixture of substrate and inhibitor revealed different binding mechanisms for E2 and S4 (Figure 1). The progress curves for S4 are linear, suggesting the binding of scFv to enzyme comes to equilibrium rapidly. Conversely, the progress curves for E2 inhibition are curved, suggesting slow binding inhibition.[30] To define the binding mechanisms of these scFvs, stopped-flow experiments were performed to evaluate the onset of inhibition during turnover at higher concentrations of enzyme. Stopped-flow experiments measured the appearance of pNA, and were carried out as described in Materials and Methods.

The stopped-flow traces from the S4 inhibitor experiments were fit by nonlinear regression to the rate equations for reversible, tight-binding inhibition to obtain observed rate constants (k_{obs}) for the onset of inhibition (equation (5)).[31] Plots of k_{obs} *versus* [S4] are linear with positive *y*-intercepts (Figure 2(a)), consistent with a one-step reversible mechanism for binding the inhibitor. The *y*-intercepts of the plots give an average off-rate of $k_{-1} = 1.7\times10^{-2}$ s^{-1}, and a secondary plot of the slopes *versus* substrate concentration (Figure 2(a), inset) defined the on rate as $k_1 = 1.2\times10^{8}$ $M^{-1}s^{-1}$. The K_I calculated from $k_{-1}/k_1 = 147$ pM, which is in very good agreement with the experimentally determined steady-state K_I of 140 pM. From these data, it can be concluded that S4 binds and inhibits MT-SP1 with an extremely fast on-rate, and has a one-step binding mechanism as shown in Scheme 1.

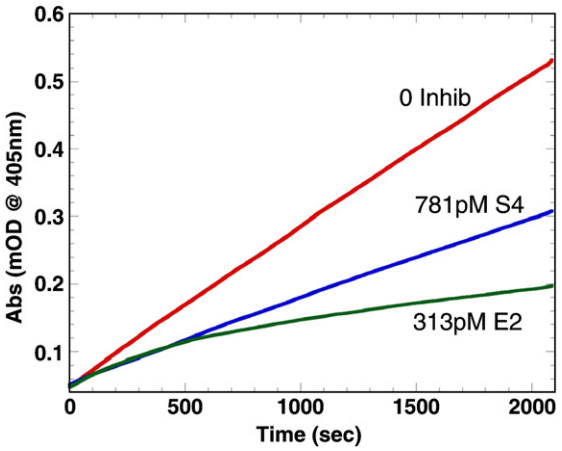

Figure 1. Progress curves of MT-SP1 inhibition by scFv inhibitors reveal multiple mechanisms of inhibition. The addition of 0.2 nM enzyme to a mixture of substrate (300 μM Spec-tPA) and inhibitor results in a decrease in proteolytic activity. S4 inhibition results in a linear progress curve, suggesting rapid-equilibrium inhibition, while the curved nature of the E2 progress curve suggests slow-binding inhibition.

Scheme 1.

The stopped-flow traces from the E2 inhibitor experiments (Figure 2(b)) revealed a more complicated binding mechanism. In this case, the progress curves fit well to a sum of two exponentials (equation (7)), indicating the presence of at least two steps in the binding process, which leads to the onset of inhibition. At minimum, a double-exponential decay is consistent with a two-step binding mechanism. This occurs when the first step in the binding process is more rapid than the second and, as a result, the first observed rate constant (k_{obs1}) shows a linear dependence on the concentration of inhibitor.[32] If k_{obs1} shows a hyperbolic dependence on inhibitor concentration, the mechanism of inhibition involves more than two steps. Unfortunately, due to the extremely tight nature of the enzyme–inhibitor interaction, the concentration of inhibitor could not be increased sufficiently to distinguish between a linear or hyperbolic dependence of k_{obs1} on the concentration of inhibitor. But, due to the presence of two exponential decays, an absolute minimal mechanism of E2 inhibition has two steps, and E2 can be classified as a slow, tight-binding inhibitor.[30]

p-Aminobenzamidine competition assay

p-Aminobenzamidine (pAB) has been reported as a weak competitive inhibitor of P1-arginine-specific serine proteases,[33] and can be used as a fluorescent probe to monitor substrate or inhibitor binding in the S1 site. The hydrophobic nature of the S1 site causes pAB to fluoresce with a maximum emission around 360 nm when bound to the enzyme, while pAB in aqueous solution has both a lower intensity and longer wavelength of emission at 376 nm. pAB has been used as a probe to monitor binding of inhibitors in the S1 site of inhibitors; competitive inhibitors displace pAB from the protease active site and reduce emission at 360 nm,[33,34] while non-competitive inhibitors do not.[35] pAB has a K_I of 28.8 μM for MT-SP1 (data not shown), and 1 μM MT-SP1 incubated with 270 μM PAB (to saturate the enzyme) shows a characteristic emission peak at 361 nm when excited at 325 nm (Figure 3). When one equivalent of either E2 or S4 is added to the pre-

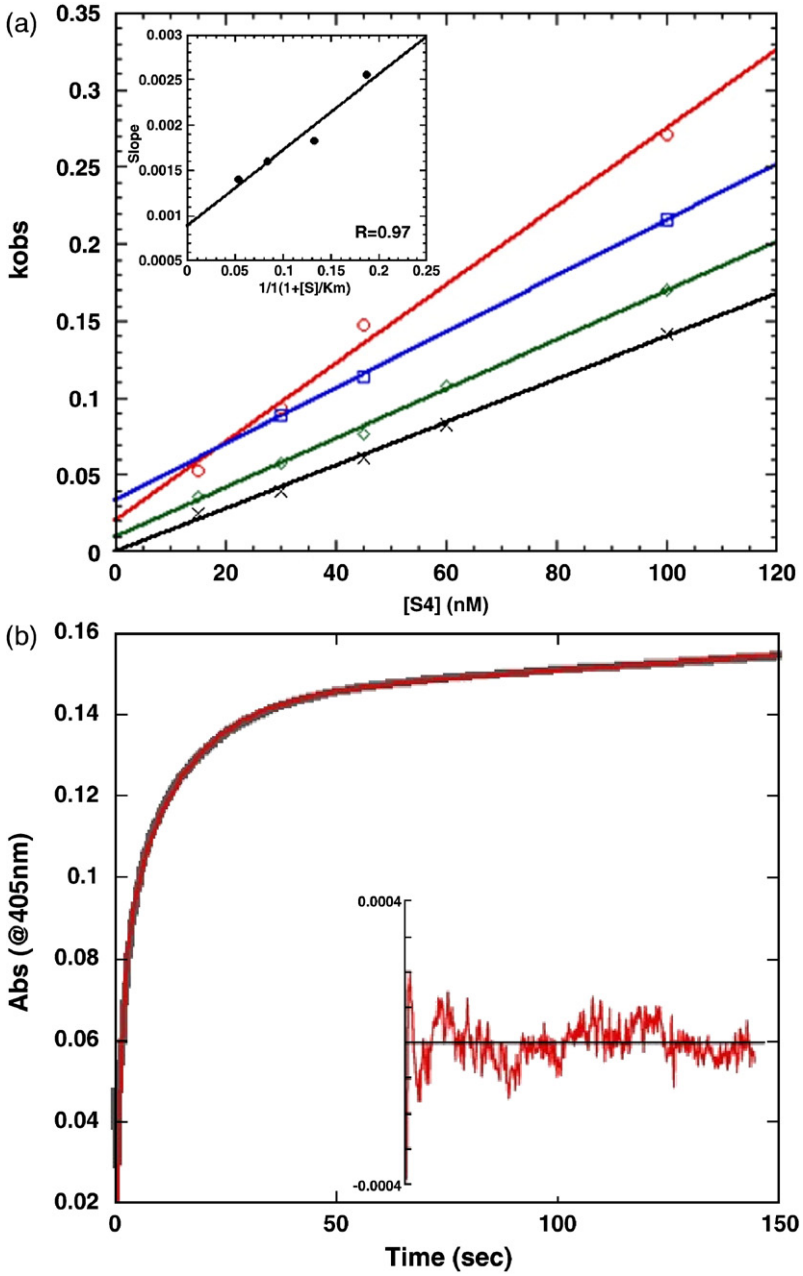

Figure 2. Stopped-flow experiments confirm disparate mechanisms of inhibitor binding to MT-SP1. (a) Linear plots of k_{obs} *versus* S4 concentration confirm that S4 has a one-step binding mechanism, as illustrated by Scheme 1. Individual traces are for different concentrations substrate: black (×), 200 μM Spec-tPA; green (◇), 300 μM Spec-tPA; blue (□), 500 μM Spec-tPA; and red (○), 800 μM Spec-tPA. The *y*-intercepts of the observed rate constant plots gave an average off rate of $k_{-1}=1.7\times10^{-2}$ s^{-1}, and a secondary plot of the slopes *versus* concentration of substrate (inset) defined the on rate as $k_1=1.2\times10^{8}$ $M^{-1}s^{-1}$. (b) The raw stopped-flow trace monitoring E2 inhibition of MT-SP1 by measuring the appearance of pNA at 405 nm fits well to the double exponential equation (7) with two observed rate constants. The inset shows the residuals of the non-linear regression fit. Final concentrations for this trace were 240 nM E2, 10 nM MT-SP1, and 500 μM Spec-tPA.

incubated MT-SP1/pAB, the fluorescence is decreased sharply (Figure 3). This suggests that both inhibitors bind at or near the S1 site, and most likely insert an arginine or lysine side-chain into the pocket.

MT-SP1/inhibitor digest

The reactive site of many standard mechanism serine protease inhibitors has been determined by incubating protease and inhibitor at low pH, where the inhibitor can be cleaved in a substrate-like manner, causing a processing of the inhibitor into two fragments, with the cleavage occurring between the P1 and P1′ residues.[36,37] When MT-SP1 and E2 are incubated at pH 6.0 for an extended period of time (>120 h), E2 is processed into two bands (Figure 4). This processing is not seen at pH 8.0, or without MT-SP1 at pH 6.0. MT-SP1 shows no proteolytic activity below pH 6.0, making this the lowest pH at which processing can occur. Electron spray ionization (ESI) mass spectrometry verifies that the processing event takes place between R131 and R132 in E2. The N-terminal fragment has a mass of 12,013 Da (expected 12,014 Da) and the C-terminal fragment has a mass of 15,624 Da (expected 15,627 Da). This places the reactive loop in the CDR3 of the heavy chain of E2, which would be expected from the HuCAL library from which these scFvs were matured, as the scaffold has large, diverse CDR3s.[29] No S4 processing was observed upon incubation with MT-SP1 for extended periods of time at low pH, suggesting a different, non-canonical mechanism of inhibition for the S4 scFv.

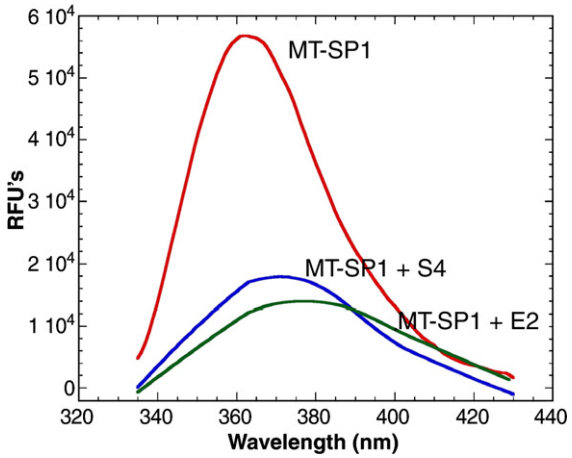

Figure 3. Inhibitors displace pAB from the MT-SP1 active site. pAB (270 μM) incubated with 1 μM MT-SP1 emits a strong emission peak with a maximum at 361 nm when excited at 325 nm, due to hydrophobic interactions between pAB and the P1 pocket of the protease. When one equivalent of either S4 (blue trace) or E2 (green trace) is added to 1 μM MT-SP1 saturated with pAB, the fluorescence decreases, suggesting pAB is released into the aqueous environment, where it is weakly fluorescent. Therefore, binding of both S4 and E2 are competitive with pAB binding, and both inhibitors bind in or near the P1 pocket in a manner that precludes binding of pAB.

Inhibitor point mutants

To verify the mechanism of inhibition of the scFv inhibitors, point mutants of the arginine residues in the CDR3 loops of the inhibitors were constructed. It would be expected that mutations to residues that bind in the S1 site of the protease would have the greatest effect on binding affinity. The mutational data are summarized in Table 2. E2 R131A and R132A had K_I values of 78 nM and 454 pM, respectively (K_I = 12.3 pM for the wild-type E2). The mutation of R131 to alanine has a 6500-fold effect on protease inhibition, as would be expected from a residue that binds in the S1 site. This is consistent with the data from the inhibitor digest at low pH. The mutation of R132 caused a 38-fold increase in K_I, suggesting that the P1′ arginine also makes significant contacts with the protease. The CDR3 loop of S4 also has a double arginine motif, R128 and R129. Both arginine residues were mutated to alanine and had significant effects on protease inhibition: S4 R128A had a K_I of 2.8 μM, while the R129 alanine mutant had a K_I of 3.9 nM, a 4×10^4-fold and a 56-fold difference, respectively.

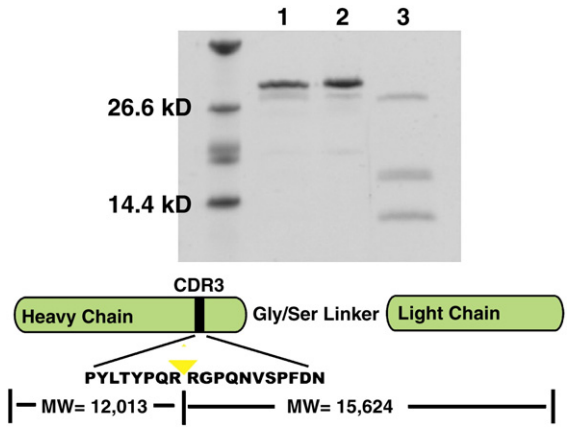

Figure 4. E2 is processed by MT-SP1 at pH 6.0. E2 (2 mM) was incubated at pH 6.0 with (lane 3) and without (lane 1) 0.1 μM MT-SP1 for 120 h. Samples were run on a 12% (w/v) polyacrylamide gel and stained with Coomassie brilliant blue. At pH 6.0, E2 was processed into two products, with molecular masses determined to be 15,624 Da, and 12,013 Da by ESI mass spectrometry. These masses, when added together, account for the mass of the full-length inhibitor (27,219 Da) and the water molecule added to the products during the hydrolysis reaction. This processing does not take place when E2 and MT-SP1 are incubated at pH 8.0 (lane2). The diagram below shows the site of the scissile bond in the middle of the heavy chain of E2.

MT-SP1 point mutations

To footprint the binding site of the inhibitors, site-directed mutagenesis was used to alanine scan the surface of the protease domain.[38] On the basis of the crystal structure of MT-SP1,[39] 30 point mutants were identified as potential partners in macromolecular interactions (Table 3). The majority of these residues were located on the loops flanking the protease active site. Proteolytic activity against Spec-tPA was used to assure that the point mutations did not drastically affect MT-SP1 structure or function. The differences between the mutant and wild-type protease k_{cat}/K_M values were less than twofold in most cases, suggesting that the mutations had minimal effect on protease structure. MT-SP1 T98A was a sixfold less efficient enzyme than the wild-type, which could be attributed primarily to a lower k_{cat}. MT-SP1 D217A had a threefold decrease in protease specific activity, which was due to an increased K_M of 210 μM. The F99A, Q192A, and W215A substitutions in MT-SP1 all resulted in inactive enzymes. The inactive variants eluted from a gel-filtration column at the same size as the zymogen protease, suggesting they are inactive because they could not autoactivate (data not shown).

The K_I values for E2 and S4 were determined against the MT-SP1 point mutants. As a positive control, the fold-specific serine protease inhibitor

Table 2. Inhibitor point mutant K_I *versus* MT-SP1

	K_I (nM)	Fold difference
E2	0.01	
E2 R131A	78	6500
E2 R132A	0.45	38
S4	0.07	
S4 R128A	2800	4.0×10^4
S4 R129A	3.9	56

All error values >6%.

Table 3. MT-SP1 point mutant/inhibitor K_I values

	BPTI		E2		S4	
	K_I (pM)	Fold difference	K_I (pM)	Fold difference	K_I (pM)	Fold difference
MT-SP1	49.7		12.3		70.4	
Q38A	20.7	0.42	6.1	0.5	73.6	1
I41A	12.4	***0.25 (fourfold)***	12.3	1	208	**3**
I60A	35.8	0.72	50.4	***4.1***	40.2	0.57
D60aA	37.2	0.75	25.1	2	125	1.8
D60bA	628	***12.6***	20.8	1.7	427	***6.1***
R60cA	134	2.7	11.4	0.93	11.7	***0.17 (sixfold)***
F60eA	24.1	0.48	11.4	0.93	102	1.4
R60fA	73.4	1.5	10.9	0.89	88.9	1.3
Y60gA	43.5	0.88	12.7	1	151	2.1
R87A	38.6	0.78	9.4	0.76	54.5	0.77
F94A	170	***3.4***	36.2	2.9	1036	***15***
N95A	83.6	1.7	45.4	***3.7***	108	1.5
D96A	150	3	>1 μM	$>10^5$	897	***13***
F97A	224	***4.5***	>1 μM	$>10^5$	154	2
T98A	76.4	1.5	83.2	***6.7***	239	***3.4***
H143A	48.5	1	14.2	1.2	1671	***24***
Q145A	83.4	1.7	15.4	1.3	116	1.6
Y146A	116	2.3	76.8	***6.2***	1405	***20***
T150A	57.8	1.2	20.1	1.6	94.6	1.3
L153A	116	2.3	21.7	1.8	116	1.6
E169A	163	***3.3***	23.1	1.9	199	2.8
Q174A	129	2.6	11.6	0.94	63.7	0.9
Q175A	39.7	0.8	851	***69***	246	***3.5***
D217A	2137	***43***	32	2.6	838	***12***
Q221aA	63.4	1.3	40.5	***3.3***	65.7	0.93
R222A	42.8	0.87	10.5	0.85	61.1	0.87
K224A	111	2.2	46.3	***3.8***	59.1	0.84

K_I is calculated from the IC_{50} value; all errors >6%.

BPTI was screened against the protease point mutants, since the mechanism of inhibition is known[40] and a the structure of a co-crystal of BPTI and MT-SP1 has been solved.[39] As would be expected from a fold-specific protease inhibitor, most point mutants had little effect on BPTI inhibition. The I41A substitution moderately improved BPTI binding to MT-SP1, F94A, F97A, and E169A moderately decreased BPTI inhibition (corresponding to <1 kcal/mol binding energy), and D60bA and D217A mutations had a more significant affect on BPTI inhibition (Figure 5(b)). Analysis of the crystal structure suggests that the increased K_I of MT-SP1 D60bA could be due to D60b hydrogen bonding with R20 of BPTI, and forming an intramolecular H-bond with R60c, which packs against BPTI. A deletion of the H-bonding ability of this side chain would account for the moderate increase (12.6-fold) in K_I. The structure does not readily explain the 43-fold increase in the K_I of BPTI for MT-SP1 D217A, but it is possible that the mutation affects the structure of the 220s loop, which would account also for the increased K_M of Spec-tPA for D217A.

The alanine scanning data suggests S4 makes contacts of moderate strength with a number of residues on the six surface loops surrounding the active site (Figure 5(a) and (d)). Interactions with the side-chains of I41, D60b, T98, and Q175 account for modest binding energy (pink residues, Figure 5(d)); alanine mutations of these residues increased the K_I values of S4 3–6 fold, corresponding to a decrease in free energy of binding of 0.5–1 kcal/mol. S4 makes stronger interactions with the side-chains of F94, D96, H143, Y146, and D217 (red residues, Figure 5(d)), decreasing the free energy of binding by 1.5–2.0 kcal/mol. Interestingly, a mutation of R60c to alanine decreased the K_I of S4 6-fold. This suggests that the protease/scFv interaction has not been optimized completely. Taken together, the mutational data suggest that S4 makes a number of moderate contacts with the loops flanking the active site, making the strongest interactions with the 140s and 90s loops, and thereby bridging the active site.

E2 makes interactions with a number of loops surrounding the MT-SP1 active site (Figure 5(c)), including the base of the 60s loop, the 90s loop, the 170s loop, the 220s loop, and the 140s loop. In contrast to S4, which makes a number of interactions of moderate strength, E2 gains much of its binding energy from interactions with two residues, D96 and F97. Mutations of each of these residues to alanine increased the K_I of E2 to >1 μM, corresponding to a decrease in free energy of binding of >7.5 kcal/mol. The Q175A variant, on the loop adjacent to the 90s loop, also has a significant effect on E2 inhibition, increasing the K_I of E2 by 69-fold (3.0 kcal/mol). The 90s loop and 170s loop flank the extended binding sites of MT-SP1,[39,41] and F97 helps form the S4 pocket, suggesting E2 binds in the extended binding pockets of MT-SP1. Though E2 makes minor interactions with Y146, Q221a, and K224, the majority of the binding energy of E2 for MT-SP1 comes from interactions with the 90s loop, and minor interactions with residues flanking the 90s

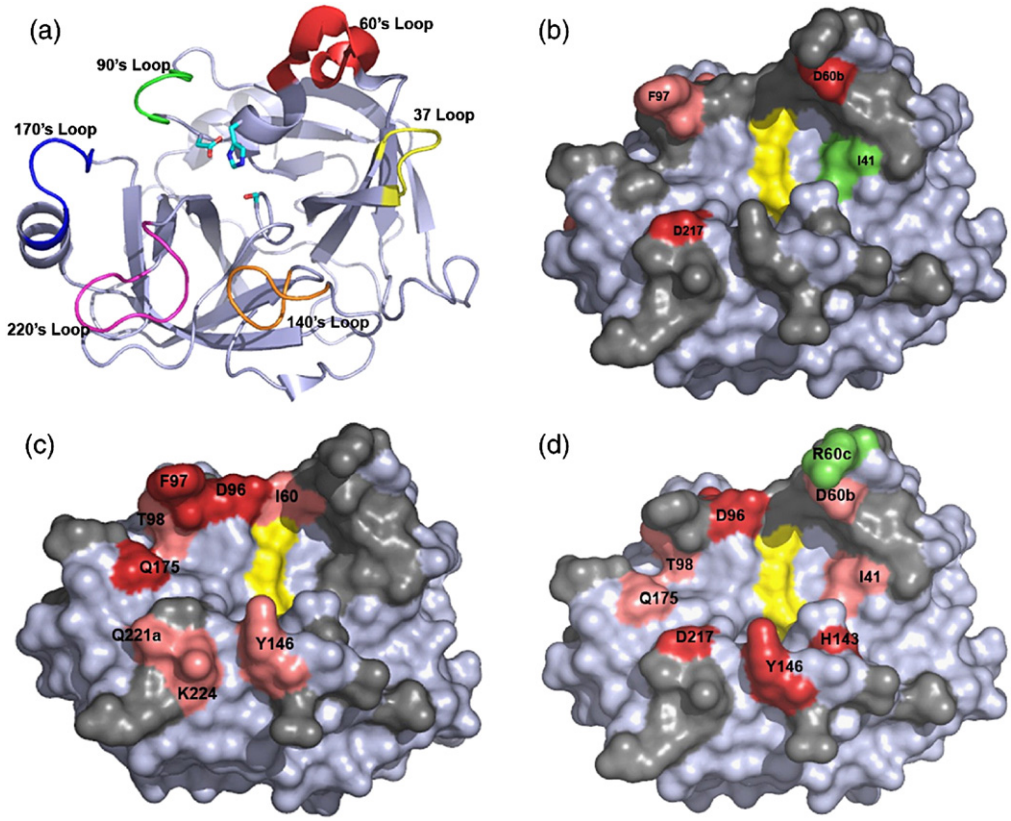

Figure 5. MT-SP1 alanine point mutants and their effect on protease inhibition by (b) BPTI, (c) E2, and (d) S4. (a) The 6 MT-SP1 surface loops surrounding the protease active site consisting of a binding cleft and the catalytic triad (sticks). The space-filling models shown in (b), (c), and (d) are oriented in the same manner, with the catalytic triad in yellow. Point mutants that had minimal effect on protease inhibition are shaded in gray, mutations that had a three-to tenfold increase in inhibitor K_I are shaded pink, and point mutants that increased inhibitor K_I by more than tenfold are shaded in red. Point mutants that decreased inhibitor K_I are shaded in green. The point-mutant/inhibitor K_I values are given in Table 3. MT-SP1 point mutants have a minimal effect on BPTI inhibition, S4 interacts with moderate affinity to all six protease loops surrounding the active site, and E2 binds with high affinity to the 90s and 170s loop. This Figure was prepared using PyMoL [http://www.pymol.sourceforge.net/].

loop (I60, Q175). This defines the 90s loop as a hot-spot for E2 binding; and as the 90s loop sequence is unique to MT-SP1, it helps explain E2s specificity for MT-SP1.

Discussion

We have described the mechanism by which two novel scFv antibodies inhibit the cancer-associated serine protease MT-SP1/matriptase. The S4 antibody has a fast association rate with MT-SP1 (1.2×10^8 $M^{-1}s^{-1}$ as measured by stopped-flow kinetics) and binds very tightly to the protease, making numerous contacts with the loops surrounding the active site of MT-SP1. The fast on-rate is likely influenced by electrostatic steering, which can increase k_{on} by more than 10^4 over the basal diffusion-controlled association rate.[42] Mutational data support this hypothesis, as nearly all the residues S4 makes significant contacts with are polar or charged. The inhibitor competes with pAB for the S1 site, and the R128A variant of S4 nearly abolishes protease inhibition. Despite these data, S4 cannot be considered a standard mechanism inhibitor of MT-SP1 without further structural characterization. Standard mechanism inhibitors have a characteristic two-step binding mechanism; an initial binding step, followed by a tightening of the enzyme–inhibitor complex and, as such, have an association rate approximately two orders of magnitude slower than S4. Furthermore, S4 is not processed by MT-SP1 at low pH, meaning the substrate-like binding cannot be assumed.

E2, on the other hand, displays all the characteristics of a standard mechanism serine protease inhibitor. While a crystal structure would help to determine the mechanism of inhibition definitively, the data here are consistent with E2 being a standard-mechanism inhibitor. The enzyme–inhibitor complex reaches equilibrium slowly, E2 binds in a substrate-like manner, and inserts an arginine residue into the S1 site of MT-SP1 (R131), which is important for, but not absolutely critical to, inhibition. Furthermore, E2 shows a slight degree of fold specificity; it inhibits the mouse homolog of MT-SP1, epithin, with a K_I of 40 nM,[24] and can inhibit trypsin, a digestive protease with extremely broad specifi-

city, with an IC_{50} of 45 μM (data not shown). In contrast to most standard mechanism serine protease inhibitors, E2 is highly specific for a single serine protease, MT-SP1. E2 gains much of its specificity through interactions with the 90s loop of MT-SP1, and makes significant interactions with residues D96 and F97 of the protease. Perhaps not surprisingly, known protease inhibitors that do exhibit a high degree of specificity, such as anticoagulant protease inhibitors from ticks and leeches, often employ a similar mechanism of inhibition; they combine the robustness of competitive, active site inhibition with protein extensions that bind to recognition sites on target enzymes.[5,43]

To our knowledge, these scFvs are the first documented case of mechanistic protease inhibitors on an antibody scaffold that bind in the active site. A number of monoclonal antibody protease inhibitors have been reported[17–19,21,22,44] but, despite diverse mechanisms, all have the same underlying mode of action; they bind to a small, linear peptide sequence and prevent either a protein–protein or an enzyme–substrate interaction. While often sufficient for inhibition, these monoclonal antibodies can have curious inhibitory profiles in which they cannot inhibit the hydrolysis of small-molecule substrates, or have different levels of inhibition against different substrates.[19,21] Because they are selected *in vitro* against the active form of the enzyme, antibodies developed by phage display have the inherent advantage of recognizing three-dimensional epitopes and the topography of the enzyme active site. With this comes the opportunity for tighter binding due to greater buried surface areas and minimal entropic penalties upon binding, and more complete inhibition through insertion of residues into the protease active site. E2 and S4 have clearly used these advantages; they have fast on-rates, very low K_D values, bind in the active site groove, and make contact with a number of loops flanking the active site.

The HuCAL-scFv library contains consensus framework sequences for all frequently occurring V_H and V_L subfamilies with a germline sequence for the CDR1 and CDR2 in each subfamily.[29] Both the heavy and light chain CDR3 regions were diversified according to the natural amino acid composition and cover the natural length variation of the V_H and V_L CDR3 regions. In retrospect, this proves to be an ideal scaffold for serine protease inhibition; it allows for a large, rigidified reactive loop to be inserted into the protease active site, while the rest of the antibody stabilizes the CDR3 of the heavy chain and makes additional contacts with the protease. While only the most potent scFv inhibitors of MT-SP1 were characterized, all inhibitors had heavy chain CDR3 loops of at least 17 residues, suggesting that large heavy chain CDR3s were critical to MT-SP1 inhibition.

The explosion in antibody research over the past 15 years has revolutionized biotechnology. Antibodies have been developed into extremely useful drugs and imaging devices, and have become critical tools in many areas of biological research. Here, scFv fragments have shown the ability to inhibit specifically a single member of a family of closely related enzymes. While these molecules will be useful in helping dissect the complex biology of MT-SP1,[45] the mechanisms through which they work once again reveals the innate binding flexibility of antibodies, and the power of protein engineering. That these inhibitors have developed the robust inhibition mechanism of standard mechanism serine protease inhibitors, suggests that we can develop antibodies to mimic any protein–protein interaction, and precisely modulate nearly any biological process.

Materials and Methods

Protein expression, purification, and mutagenesis

MT-SP1 and MT-SP1 mutants were expressed in *Escherichia coli* and purified from inclusion bodies as described.[25] Antibodies were selected from the HuCAL scFv library (MorphoSys AG, Martinsried, Germany).[29] Expression and purification of inhibitory scFv antibodies were as described.[24] Point mutants were made using the Stratagene Quickchange kit (Stratagene, La Jolla, CA). One or two base changes were sufficient to create the point mutant in each case, and all sequences were verified by DNA sequencing.

Steady-state kinetics

All reaction volumes were 120 μl and were carried out in 50 mM Tris–HCl (pH 8.8), 50 mM NaCl, 0.01% (v/v) Tween-20 unless stated otherwise and all reactions were carried out in triplicate. Reactions were run in 96-well, medium-binding, flat-bottomed plates (Corning), and cleavage of substrate was measured with a UVmax Microplate Reader (Molecular Devices Corporation, Palo Alto, CA.). MT-SP1 and mutant protease concentrations were determined by 4-methylumbelliferyl *p*-guanidinobenzoate active-site titration with a Fluormax-2 spectrofluorimeter.[46] Kinetic parameters of MT-SP1 and mutant proteases were determined at 0.2 nM enzyme, with concentrations of Spectrazyme-tPA (hexahydrotyrosyl-Gly-Arg-pNA, American Diagnostica, Greenwich, CT) varying from 1 μM to 400 μM. K_M and k_{cat} were determined using the Michaelis–Menten equation.

Tight-binding inhibitors require that the effective decrease in free enzyme be taken into account when determining K_I values.[31] This is accomplished by incubating enzyme and inhibitor so that the system can reach equilibrium, adding substrate, and then measuring steady-state velocities at various concentrations of inhibitor and fitting the data to:

$$v_i/v_s = \left\{ \frac{[E_T - I_T - K_I^*] + [(I_T + K_I^* - E_T)^2 + (4K_I^* E_T)]^{1/2}}{2E_T} \right\} \quad (1)$$

K_I^* values are then plotted against substrate concentration to extrapolate the K_I at zero substrate concentration:

$$K_I^* = K_I(1 + [S]/K_m) \quad (2)$$

When measuring the effect mutations had on the strength of the interaction between the protease and inhibitor, IC_{50} values were used instead of K_I as determined above. Though less accurate than K_I,[47] IC_{50} is easier to calculate when screening large numbers of inhibitor point mutants, and is sufficient to monitor relative changes in inhibition *versus* the wild-type system. IC_{50} was determined by incubating inhibitor and 0.2 nM enzyme for at least 5 h at room temperature to assure steady-state behavior of the system.[3] There was no appreciable decrease in protease activity during the incubation period. Steady-state velocities were then plotted against inhibitor concentration and fit to:

$$v = v_{min} + \frac{(v_{max} - v_{min})}{(1 + 10^{([I]-IC_{50})})} \quad (3)$$

Relative K_I was calculated from IC_{50} values according to:

$$K_I = \frac{IC_{50}}{(1 + [S]/K_M)} \quad (4)$$

Though nearly all protease mutants had a minimal (less than twofold) effect on substrate K_M, and the substrate concentration was held well above the K_M, this correction normalizes the IC_{50} with respect to the strength of the protease/substrate interaction. All graphs and equations were fit using Kaliedagraph 3.6 (Synergy Software, Reading, PA).

Macromolecular substrate assay

In an assay analogous to that used to monitor factor VIIa activation of FX,[8] we developed a coupled assay that monitors MT-SP1 activation of uPA in which 50 pM MT-SP1 was incubated with various concentrations (final concentrations, 12.5–400 nM) of single-chain uPA (American Diagnostica). At various time-points (0–150 min), aliquots of the reaction were removed and quenched with 10 nM E2. There was no residual MT-SP1 activity after the quench, and E2 showed no inhibition of uPA at a concentration of 10 nM. The amount of active uPA was measured by monitoring the activity for uPA against the *para*-nitroanilide uPA substrate Spectrazyme-UK (American Diagnostica). The mode of inhibition was determined from double reciprocal plots, and kinetic parameters and inhibition constants were determined using the Michaelis–Menten equation. The K_M of Spec-UK for uPA was determined to be 42 μM, and the k_{cat} of uPA turnover was 1.0 s^{-1}.

Stopped-flow kinetics

Stopped-flow experiments were conducted using a HiTech SF-61DX2 instrument (TgK Scientific Ltd., Bradford on Avon, U.K.). Data were collected in dual beam mode using photomultiplier detection of absorbance data at 405 nm. MT-SP1 (10 nM for E2 experiments, 1 nM for S4 experiments) was mixed rapidly with a solution of substrate (Spec-tPA, 200–800 μM) and inhibitor (10–300 nM for S4, 100–340 nM for E2) and the appearance of pNA was monitored for 20 s (for S4) or 150 s (for E2). Concentrations of enzyme and length of experiments were varied between the two systems to ensure robust signal and equilibration of the system.

The stopped-flow traces from the S4 inhibitor experiments were fit by nonlinear regression to the rate equations for reversible, tight binding inhibition:[31]

$$P = v_s t + (v_i - v_s)(1 - e^{-k_{obs}t})/k_{obs} \quad (5)$$

The appearance of the product (P) is a function of the initial (v_i) and final (v_s) velocities, and an apparent first-order rate constant, k_{obs} for the onset of inhibition. Plots of k_{obs} *versus* inhibitor concentration were linear, and fit to equation (6), as would be expected when the inhibitory mechanism consists of one reversible binding step, as in Scheme 1:

$$k_{obs} = k_{-1} + k_1[I]/(1 + [S]/K_M) \quad (6)$$

E2 stopped-flow traces fit poorly to equation (5), but fit well to a mechanism with two observed rate constants:[32]

$$P = v_s t + (v_i - v_s)(1 - e^{-k_{obs1}t})/k_{obs1} + (v_i - v_s)(1 - e^{-k_{obs2}t})/k_{obs2} \quad (7)$$

p-Aminobenzamidine fluorescence

Experiments were carried out in PBS with a Fluorolog 3 (Instruments SA Inc. Edison, NJ) fluorimeter. Emission spectra of MT-SP1/pAB were obtained by excitation at 325 nm using a 4 nm excitation and 2 nm emission bandpass, and were scanned from 335–430 nm. Spectra were corrected for emission due to free pAB and protease. Data corrections were performed with Datamax 2.20 software (Instruments SA).

Inhibitor digest

E2 (2 μM) or S4 (2 μM) was incubated with 0.1 nM MT-SP1 for 120 h at room temperature. Proteins were incubated in 100 mM Mes (pH 6.0), 100 mM NaCl or in 50 mM Tris–HCl (pH 8.0), 100 mM NaCl. Proteolysis was monitored by gel mobility-shift on a 12% (w/v) polyacrylamide gel with a 4.5% stacking gel, and stained with Coomassie brilliant blue. ESI mass spectrometry was carried out with an LCT Premier mass spectrometer (Waters Corp. Milford, MA), and molecular masses were determined using MassLynx (Waters) deconvolution software.

Acknowledgements

We thank Jill Winter (Chiron) and MorphoSys AG for access to the HuCAL-scFv libraries, and Dr Ami Bhatt, Dr Alan Marnett, and Dr Sami Mahrus for many helpful discussions. This work was funded by a Program Project Grant for proteases in cancer, NIH CA72006 (to C.S.C.), the Department of Defense Breast Cancer Research Program BC043431 (C.J.F.) and NIH training grant GM08284 (M.R.D.). HuCAL is a registered trademark of MorphoSys AG.

References

1. Rawlings, N. D., Morton, F. R. & Barrett, A. J. (2006). MEROPS: the peptidase database. *Nucl. Acids Res.* **34**, D270–D272.
2. Laskowski, M., Jr & Kato, I. (1980). Protein inhibitors of proteinases. *Annu. Rev. Biochem.* **49**, 593–626.
3. Eggers, C. T., Wang, S. X., Fletterick, R. J. & Craik, C. S. (2001). The role of ecotin dimerization in protease inhibition. *J. Mol. Biol.* **308**, 975–991.
4. Tyndall, J. D., Nall, T. & Fairlie, D. P. (2005). Proteases universally recognize beta strands in their active sites. *Chem. Rev.* **105**, 973–999.
5. Rydel, T. J., Tulinsky, A., Bode, W. & Huber, R. (1991). Refined structure of the hirudin-thrombin complex. *J. Mol. Biol.* **221**, 583–601.
6. Castro, M. J. & Anderson, S. (1996). Alanine point-mutations in the reactive region of bovine pancreatic trypsin inhibitor: effects on the kinetics and thermodynamics of binding to beta-trypsin and alpha-chymotrypsin. *Biochemistry*, **35**, 11435–11446.
7. Coussens, L. M., Fingleton, B. & Matrisian, L. M. (2002). Matrix metalloproteinase inhibitors and cancer: trials and tribulations. *Science*, **295**, 2387–2392.
8. Dennis, M. S., Eigenbrot, C., Skelton, N. J., Ultsch, M. H., Santell, L., Dwyer, M. A. *et al.* (2000). Peptide exosite inhibitors of factor VIIa as anticoagulants. *Nature*, **404**, 465–470.
9. Roberge, M., Santell, L., Dennis, M. S., Eigenbrot, C., Dwyer, M. A. & Lazarus, R. A. (2001). A novel exosite on coagulation factor VIIa and its molecular interactions with a new class of peptide inhibitors. *Biochemistry*, **40**, 9522–9531.
10. Krook, M., Lindbladh, C., Eriksen, J. A. & Mosbach, K. (1997). Selection of a cyclic nonapeptide inhibitor to alpha-chymotrypsin using a phage display peptide library. *Mol. Divers.* **3**, 149–159.
11. Hansen, M., Wind, T., Blouse, G. E., Christensen, A., Petersen, H. H., Kjelgaard, S. *et al.* (2005). A urokinase-type plasminogen activator-inhibiting cyclic peptide with an unusual P2 residue and an extended protease binding surface demonstrates new modalities for enzyme inhibition. *J. Biol. Chem.* **280**, 38424–38437.
12. Wang, C. I., Yang, Q. & Craik, C. S. (1995). Isolation of a high affinity inhibitor of urokinase-type plasminogen activator by phage display of ecotin. *J. Biol. Chem.* **270**, 12250–12256.
13. Dennis, M. S. & Lazarus, R. A. (1994). Kunitz domain inhibitors of tissue factor-factor VIIa. II. Potent and specific inhibitors by competitive phage selection. *J. Biol. Chem.* **269**, 22137–22144.
14. Stoop, A. A. & Craik, C. S. (2003). Engineering of a macromolecular scaffold to develop specific protease inhibitors. *Nature Biotechnol.* **21**, 1063–1068.
15. Binz, H. K., Amstutz, P., Kohl, A., Stumpp, M. T., Briand, C., Forrer, P. *et al.* (2004). High-affinity binders selected from designed ankyrin repeat protein libraries. *Nature Biotechnol.* **22**, 575–582.
16. Rezacova, P., Lescar, J., Brynda, J., Fabry, M., Horejsi, M., Sedlacek, J. & Bentley, G. A. (2001). Structural basis of HIV-1 and HIV-2 protease inhibition by a monoclonal antibody. *Structure*, **9**, 887–895.
17. Puchi, M., Quinones, K., Concha, C., Iribarren, C., Bustos, P., Morin, V. *et al.* (2006). Microinjection of an antibody against the cysteine-protease involved in male chromatin remodeling blocks the development of sea urchin embryos at the initial cell cycle. *J. Cell Biochem.* **98**, 335–342.
18. Fukuoka, Y. & Schwartz, L. B. (2006). The B12 anti-tryptase monoclonal antibody disrupts the tetrameric structure of heparin-stabilized beta-tryptase to form monomers that are inactive at neutral pH and active at acidic pH. *J. Immunol.* **176**, 3165–3172.
19. Petersen, H. H., Hansen, M., Schousboe, S. L. & Andreasen, P. A. (2001). Localization of epitopes for monoclonal antibodies to urokinase-type plasminogen activator: relationship between epitope localization and effects of antibodies on molecular interactions of the enzyme. *Eur. J. Biochem.* **268**, 4430–4439.
20. Matias-Roman, S., Galvez, B. G., Genis, L., Yanez-Mo, M., de la Rosa, G., Sanchez-Mateos, P. *et al.* (2005). Membrane type 1-matrix metalloproteinase is involved in migration of human monocytes and is regulated through their interaction with fibronectin or endothelium. *Blood*, **105**, 3956–3964.
21. Xuan, J. A., Schneider, D., Toy, P., Lin, R., Newton, A., Zhu, Y. *et al.* (2006). Antibodies neutralizing hepsin protease activity do not impact cell growth but inhibit invasion of prostate and ovarian tumor cells in culture. *Cancer Res.* **66**, 3611–3619.
22. Obermajer, N., Premzl, A., Zavasnik Bergant, T., Turk, B. & Kos, J. (2006). Carboxypeptidase cathepsin X mediates beta2-integrin-dependent adhesion of differentiated U-937 cells. *Expt. Cell Res.* **312**, 2515–2527.
23. Maun, H. R., Eigenbrot, C. & Lazarus, R. A. (2003). Engineering exosite peptides for complete inhibition of factor VIIa using a protease switch with substrate phage. *J. Biol. Chem.* **278**, 21823–21830.
24. Sun, J., Pons, J. & Craik, C. S. (2003). Potent and selective inhibition of membrane-type serine protease 1 by human single-chain antibodies. *Biochemistry*, **42**, 892–900.
25. Takeuchi, T., Shuman, M. A. & Craik, C. S. (1999). Reverse biochemistry: use of macromolecular protease inhibitors to dissect complex biological processes and identify a membrane-type serine protease in epithelial cancer and normal tissue. *Proc. Natl Acad. Sci. USA*, **96**, 11054–110561.
26. Lin, C. Y., Anders, J., Johnson, M. & Dickson, R. B. (1999). Purification and characterization of a complex containing matriptase and a Kunitz-type serine protease inhibitor from human milk. *J. Biol. Chem.* **274**, 18237–18242.
27. Uhland, K. (2006). Matriptase and its putative role in cancer. *Cell Mol. Life Sci.* **63**, 2968–2978.
28. List, K., Szabo, R., Molinolo, A., Sriuranpong, V., Redeye, V., Murdock, T. *et al.* (2005). Deregulated matriptase causes ras-independent multistage carcinogenesis and promotes ras-mediated malignant transformation. *Genes Dev.* **19**, 1934–1950.
29. Knappik, A., Ge, L., Honegger, A., Pack, P., Fischer, M., Wellnhofer, G. *et al.* (2000). Fully synthetic human combinatorial antibody libraries (HuCAL) based on modular consensus frameworks and CDRs randomized with trinucleotides. *J. Mol. Biol.* **296**, 57–86.
30. Morrison, J. F. & Walsh, C. T. (1988). The behavior and significance of slow-binding enzyme inhibitors. *Advan. Enzymol. Relat. Areas Mol. Biol.* **61**, 201–301.
31. Williams, J. W. & Morrison, J. F. (1979). The kinetics of reversible tight-binding inhibition. *Methods Enzymol.* **63**, 437–467.
32. Hiromi, K. (1979). *Kinetics of Fast Enzyme Reaction: Theory and Pratice.* Kodansha Ltd., Wiley, Tokyo.
33. Evans, S. A., Olson, S. T. & Shore, J. D. (1982). *p*-Aminobenzamidine as a fluorescent probe for the active site of serine proteases. *J. Biol. Chem.* **257**, 3014–3017.
34. Parry, M. A., Maraganore, J. M. & Stone, S. R. (1994).

Kinetic mechanism for the interaction of Hirulog with thrombin. *Biochemistry*, **33**, 14807–14814.
35. Fernandez, A. Z., Tablante, A., Beguin, S., Hemker, H. C. & Apitz-Castro, R. (1999). Draculin, the anticoagulant factor in vampire bat saliva, is a tight-binding, noncompetitive inhibitor of activated factor X. *Biochim. Biophys. Acta*, **1434**, 135–142.
36. Ozawa, K. & Laskowski, M., Jr (1966). The reactive site of trypsin inhibitors. *J. Biol. Chem.* **241**, 3955–3961.
37. McGrath, M. E., Hines, W. M., Sakanari, J. A., Fletterick, R. J. & Craik, C. S. (1991). The sequence and reactive site of ecotin. A general inhibitor of pancreatic serine proteases from *Escherichia coli*. *J. Biol. Chem.* **266**, 6620–6625.
38. Cunningham, B. C. & Wells, J. A. (1989). High-resolution epitope mapping of hGH-receptor interactions by alanine-scanning mutagenesis. *Science*, **244**, 1081–1085.
39. Friedrich, R., Fuentes-Prior, P., Ong, E., Coombs, G., Hunter, M., Oehler, R. *et al.* (2002). Catalytic domain structures of MT-SP1/matriptase, a matrix-degrading transmembrane serine proteinase. *J. Biol. Chem.* **277**, 2160–2168.
40. Luthy, J. A., Praissman, M., Finkenstadt, W. R. & Laskowski, M., Jr (1973). Detailed mechanism of interaction of bovine-trypsin with soybean trypsin inhibitor (Kunitz). I. Stopped flow measurements. *J. Biol. Chem.* **248**, 1760–1771.
41. Sriprapundh, D., Craik, C. S. (2006).
42. Schreiber, G. & Fersht, A. R. (1996). Rapid, electrostatically assisted association of proteins. *Nature Struct. Biol.* **3**, 427–431.
43. Rezaie, A. R. (2004). Kinetics of factor Xa inhibition by recombinant tick anticoagulant peptide: both active site and exosite interactions are required for a slow- and tight-binding inhibition mechanism. *Biochemistry*, **43**, 3368–3375.
44. Martin, F., Volpari, C., Steinkuhler, C., Dimasi, N., Brunetti, M., Biasiol, G. *et al.* (1997). Affinity selection of a camelized V(H) domain antibody inhibitor of hepatitis C virus NS3 protease. *Protein Eng.* **10**, 607–614.
45. Bhatt, A. S., Welm, A., Farady, C. J., Vasquez, M., Wilson, K. & Craik, C. S. (2007). Coordinate expression and functional profiling identify and extracellular proteolytic signaling pathway. *Proc. Natl Acad. Sci. USA*, **104**, 5771–5776.
46. Jameson, G. W., Roberts, D. V., Adams, R. W., Kyle, W. S. & Elmore, D. T. (1973). Determination of the operational molarity of solutions of bovine alpha-chymotrypsin, trypsin, thrombin and factor Xa by spectrofluorimetric titration. *Biochem. J.* **131**, 107–117.
47. Chou, T. (1974). Relationships between inhibition constants and fractional inhibition in enzyme-catalyzed reactions with different numbers of reactants, different reaction mechanisms, and different types and mechanisms of inhibition. *Mol. Pharmacol.* **10**, 235–247.

Edited by I. Wilson

(Received 23 February 2007; accepted 20 March 2007)
Available online 4 April 2007